Astron. Astrophys. 317, 203–211 (1997)

ASTRONOMY AND ASTROPHYSICS

Neutral hydrogen compact absorption features in Cassiopeia A

E.M. Reynoso[1,*], **W.M. Goss**[2], **G.M. Dubner**[1,**], **P.F. Winkler**[3,***], **U.J. Schwarz**[4]

[1] Instituto de Astronomía y Física del Espacio, C.C.67, Suc. 28, 1428 Buenos Aires, Argentina (ereynoso@iafe.uba.ar)
[2] National Radio Astronomy Observatory, Very Large Array, P.O. Box 0, Socorro, New Mexico 87801, USA
[3] Department of Physics, Middlebury College, Middlebury, VT 05753, USA
[4] Kapteyn Astronomical Institute, Postbus 800, NL-9700 AV Groningen, The Netherlands

Received 2 April 1996 / Accepted 2 May 1996

Abstract. Very Large Array (VLA) observations of the $\lambda 21$ cm H I line towards Cassiopeia A (Cas A) have been performed. The velocity interval observed was from -38 to -362 (LSR) km s^{-1}, with a resolution of 2.6 km s^{-1} and a beam size of $14.2'' \times 11.4''$. Opacity images show the presence of a number of small absorption H I features in the velocity interval -62 to -69 km s^{-1} (LSR) which, on the basis of several arguments, are postulated to be physically associated with Cas A. These cold H I knots have sizes of < 0.1 pc and show spatial substructure. Their velocities lie well outside the range of the intervening H I in the Perseus spiral arm, i.e. 0 to -55 km s^{-1}. We demonstrate that the H I knots cannot be described as shocked interstellar cloudlets engulfed by the blast wave of the supernova remnant (SNR). Instead, we propose that these low velocity H I features are recombined wind driven clumps moving ahead of the supernova (SN) shock front. This hypothesis is supported by the ages derived for the knots, varying from 8×10^3 to 5×10^4 years, which implies that these features were originally accelerated during the Wolf-Rayet (WR) phase of the precursor star.

Key words: ISM: supernova remnants – ISM: individual: Cas A – stars: mass loss

1. Introduction

Cassiopeia A (Cas A) is a young galactic supernova remnant (SNR) which is thought to be the debris of a very massive WN star that exploded as a type II supernova (Fesen et al. 1987). It is believed that the supernova event which gave rise to Cas A could have been observed by Flamsteed in 1680 (Ashworth 1980).

This SNR has been intensively studied throughout the whole electromagnetic spectrum. At radio and X-ray wavelengths, the remnant appears as a bright ring of clumpy emission surrounded by an approximately circular region of diffuse emission. The optical emission from Cas A consists of a faint, incomplete shell with a protrusion at the north-east, and a number of clumps which can be classified into two major groups, according to their kinematics and composition: the fast moving knots (FMKs), with spatial velocities between 4000 and 8000 km s^{-1}, and the quasi-stationary flocculi (QSFs), with velocities of about 200 km s^{-1}. The kinematics of the FMKs and QSFs has been investigated in detail by van den Bergh and Kamper (van den Bergh 1971; Kamper & van den Bergh 1976; van den Bergh & Kamper 1983, 1985), based on nearly four decades of observations. Reed et al. (1995) have recently reported the detection of 3663 FMKs and 450 QSFs.

The FMKs are rich in oxygen and the silicon-group elements. None of them emits in hydrogen, helium or nitrogen (Peimbert & van den Bergh 1971; Chevalier & Kirshner 1978, 1979). On the other hand, the QSFs contain mainly nitrogen and hydrogen. The QSFs are thought to be the remnants of the outer layer of the progenitor star, which were lost prior to the explosion. Most of the QSFs are blue-shifted, and do not appear to lie on an expanding shell (Reed et al. 1991). There exists a third group, the so-called "fast-moving flocculi", consisting of knots with velocities similar to the FMKs but having the chemical composition of QSFs (Fesen et al. 1987). Based on 74 and 333 MHz data, Kassim et al. (1995) detected a free-free absorption component towards the center of Cas A which may be related to unshocked ejecta expanding freely within the boundaries of the reverse shock.

Radio continuum observations of Cas A also reveal the presence of bright emission knots lying within the boundaries of the diffuse radio shell. Bell (1977) measured proper motions for 30 compact radio knots using the Cambridge 5-km radio telescope at 5 GHz, and concluded that the radio knots are in random motion. Tuffs (1986) found 342 distinct radio peaks, with sizes ranging from 1 arcmin to less than the beam size of $\sim 2.0''$, which are moving systematically from a point offset to the NW

Send offprint requests to: Estela M. Reynoso
[*] Fellowship of CONICET, Argentina
[**] Member of the Carrera del Investigador Científico of CONICET, Argentina.
[***] Visiting Astronomer, Kitt Peak National Observatory, which is operated by the Association of Universities for Research in Astronomy under contract to the National Science Foundation.

with respect to the center of expansion of the optical FMKS. Anderson & Rudnick (1995) combined observations made with the Cambridge telescope and the VLA spanning a time range of 12 years, and concluded that a range of dynamical conditions apply to the radio knots and to the bulk motion of the radio plasma. The characteristic timescale of expansion for compact features in the bright radio ring in Cas A is about 950 years; outside the ring, timescales vary from 900 to 550 years. On the other hand, expansion ages of 750 years (north-south) and 1300 years are obtained for the diffuse radio emitting component.

By comparing radio and soft X-ray observations, Keohane et al. (1996) concluded that the thermal and relativistic plasmas occupy the same volumes and share common physical parameters. They also suggest a physical connection between Cas A and a molecular cloud lying towards the west at a velocity of $-40\,\mathrm{km\ s^{-1}}$.

X-ray line observations of Si XIII, S XV and S XVI (Markert et al. 1983) show that the emission is redshifted to the northwest and blueshifted to the southeast. These observations suggest that most of the radiation from the northwest region originates on the far side of Cas A, while the southeastern emission may arise from an approaching arc on the near side. Markert et al. (1983) interpret these results by modelling the X-ray emitting gas as a clumpy ring inclined with respect to the observer. Such a tilted ring model is also proposed by Kenney & Dent (1985) based on differences between spectral indices and rotation measures at 86 GHz.

Using the 100-m Effelsberg radio telescope, Mebold & Hill (1975) detected a small H I absorption feature at a velocity of $-65\,\mathrm{km\ s^{-1}}$ in the direction of Cas A with a $9'$ beam. Goss et al. (1988) observed this feature using the Westerbork Synthesis Radio Telescope (WSRT), with a synthesized beam of $27'' \times 32''$ and a velocity resolution of $0.62\,\mathrm{km\ s^{-1}}$. The proximity of the H I feature to three prominent QSFs suggested an association among them. Goss et al. (1988) proposed that the H I feature could be a cold, recombined, high density QSF as suggested by McKee & Cowie (1975).

In this paper we present $\lambda 21$ cm VLA[1] observations in the velocity range -38 to $-362\,\mathrm{km\ s^{-1}}$, performed in order to search for additional high velocity H I features. A major goal is to investigate the interaction of the different components observed in Cas A with the surrounding interstellar medium. The study is performed through absorption features because they are readily apparent against the strong radio continuum background provided by Cas A. Such a sensitive experiment is possible only for very few bright SNRs.

2. Observations

2.1. Radio observations

Cas A was observed with the VLA for 6 hours on 1993 July 30 in the C array and for 7 hours on 1993 September 2 during the move from the C to the D array. The number of velocity channels used was 127 centered at $-200\,\mathrm{km\ s^{-1}}$ (LSR), with a velocity resolution of $2.6\,\mathrm{km\ s^{-1}}$. The velocity interval was selected in order to avoid the stronger contribution of galactic plane H I, approximately confined between 0 and $-55\,\mathrm{km\ s^{-1}}$ in this direction of the galaxy. This velocity range allows the detection of only blue-shifted H I features. The synthesized beam is $14.2'' \times 11.4''$, with a position angle of 38°. The total flux density in the continuum image is 1850 ± 50 Jy. The continuum r.m.s. noise level is 60 mJy/beam (limited by dynamic range due to the intense continuum), while the line channels have an r.m.s. noise of 13 mJy/beam.

Opacity maps in H I were calculated as $\tau = -\ln(T_b/T_c + 1)$, where the ratio inside the parenthesis was estimated by dividing each H I channel by the continuum image. The sensitivity in τ is $\sim 0.009(3\sigma)$. A continuum cut-off of 1 Jy/beam (6% of the peak of 16 Jy/beam) was used in order to avoid edge effects, where the continuum emission drops abruptly. At the edge of the source, the 1 sigma detection limit in opacity is 0.007.

2.2. Optical observations

The optical QSFs are illustrated in the image shown in Fig. 1. Cas A was observed from the 4-m telescope and a TI CCD at KPNO in 1986 September. Observations were made through a 50 Å bandpass interference filter centered at 6563 Å, a bandpass which admits both Hα and the [N II] $\lambda\lambda$ 6548, 6583 lines, all of which are prominent in the QSFs. Four overlapping fields were observed through a 100 Å bandpass continuum filter centered at 6100 Å. Each set of images was processed and combined into a mosaic, and the continuum image was scaled and subtracted to remove most of the stars and make the QSFs more readily apparent. The result is shown in Fig. 1. The numbers on the figure refer to the features detected in H I absorption, and these are discussed below.

3. Results

The resulting H I opacity images show a prominent peak in τ near $-48\,\mathrm{km\ s^{-1}}$, which is observed over a great deal of the source. This peak is related to optically thick H I in the range -45 to $-54\,\mathrm{km\ s^{-1}}$, originating in the Perseus arm (Bieging et al. 1991). Thus, in order to investigate the neutral gas possibly associated with Cas A, the current data have been analyzed for velocities more negative than $-54\,\mathrm{km\ s^{-1}}$.

After direct inspection over each optical depth image throughout the whole area stubtended by Cas A, we selected a number of high velocity H I absorption features similar to the one imaged by Goss et al. (1988). In order to select the candidates, we required that the features be statistically significant in all three coordinates (RA, Dec and velocity). Features for which either the spatial or the velocity peak were not prominent were still retained and labelled with a question mark.

The selected set includes a total of 17 absorption features, all with LSR velocities in the range -62 to $-69\,\mathrm{km\ s^{-1}}$.

[1] The Very Large Array of the National Radio Astronomy Observatory is a facility of the National Science Foundation operated under cooperative agreement by Associated Universities, Inc.

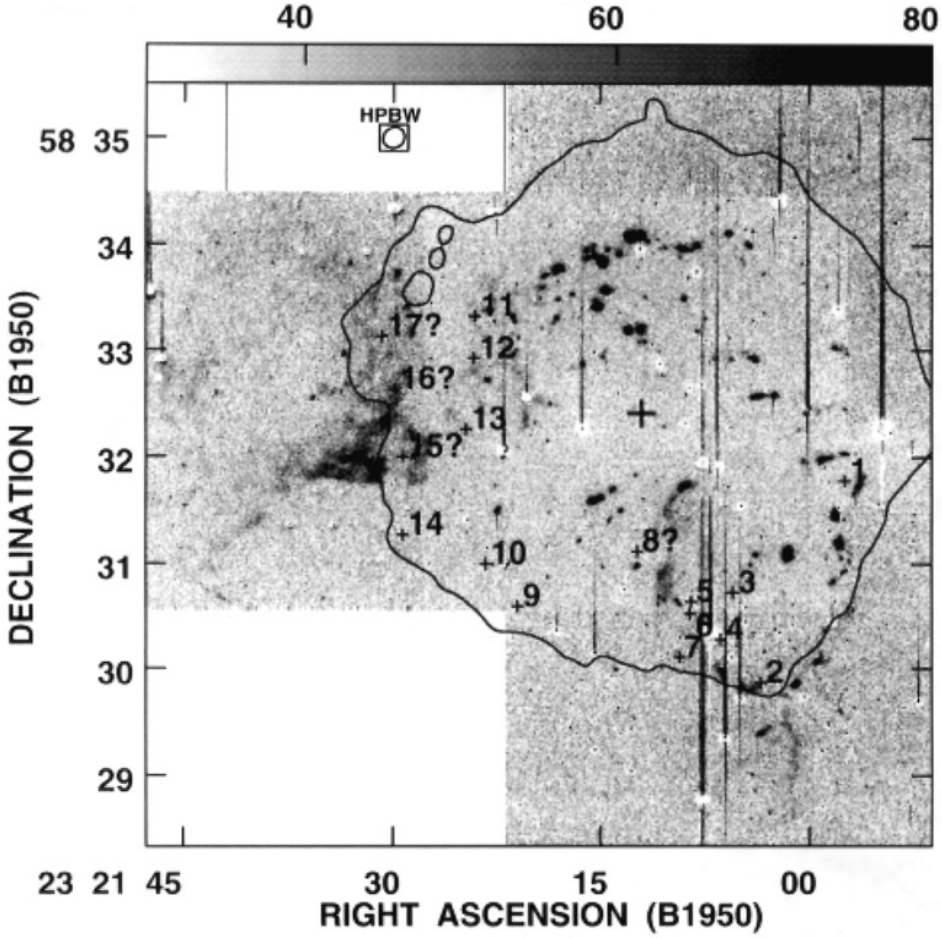

Fig. 1. Hα image of Cas A. The crosses indicate the positions of the H I absorption features. Features labelled with a question mark satisfy only one of the selection criteria (see text). The beamsize of the λ21 cm observations is shown in the upper blanked portion of the image. The big plus sign at the center indicates the position of the assumed geometric center, at RA(1950) = $23^{\rm h}21^{\rm m}12.0^{\rm s}$, Dec(1950) = $+58^\circ32'24''$. The 1420 MHz continuum contour at 1 Jy/beam is included

The presence of the feature detected with the WSRT around $\alpha(1950) = 23^{\rm h}21^{\rm m}8.5^{\rm s}$, $\delta(1950) = +58^\circ30'38''$ was confirmed. No features were found at velocities comparable to those of the QSFs, i.e. from about -100 to the limit of -350 km s^{-1}.

Figure 2 shows the distribution of the H I knots over Cas A superimposed on the radio continuum greyscale image. The H I absorption features are indicated with crosses. The numbers correspond to the names in Table 1. We compared the H I absorption features with WSRT observations (Schwarz et al. 1996), which have angular and velocity resolutions of about $50''$ and 0.62 km s^{-1} respectively. These observations span from -105 km s^{-1} to 23 km s^{-1}. Although the resolutions differ much from the present observations, rough agreement exists for most of the features.

Figure 3 shows the opacity profiles for the 17 features. Only for the purpose of comparison, plot number 18 shows the profile obtained towards an arbitrary direction in Cas A, at $\alpha(1950) = 23^{\rm h}21^{\rm m}10.0^{\rm s}$, $\delta(1950) = +58^\circ33'21''$. At the extreme left of the profiles (-52 km s^{-1}), the opacity tends to increase, due to the Perseus arm absorption feature (Bieging et al. 1991). Figure 4 illustrates the spatial cuts towards some of the H I knots.

With the present resolution, the detection of substructure within individual H I knots is possible. For instance, the H I feature reported by Goss et al. (1988) with a resolution of $\sim 30''$ consists in fact of two features, knots 5 and 6. Feature 5 is resolved with our $\sim 12''$ resolution, while feature 6 appears as a point source.

Other features with double or irregular substructure are features 1, 2, 7, 9, 10, 13, 15 and 17. For some features, the boundaries cannot be well established and thus the sizes are uncertain. Also, the H I features 8, 16 and 17 are spatially distinct but the signal-to-noise ratio of the profiles is $< 3\sigma$. For the sake of completeness, the features labelled with a question mark were included in Figs. 2 and 3; the best estimates of their parameters are listed in Table 1. However, since their association with Cas A is uncertain, they are not considered in the statistical study.

The list of the features with both observed and derived parameters is shown in Table 1. The first column is the name of each feature. Columns 2 to 4 list the epoch 1993 position, measured in 1950 equatorial coordinates and in seconds of arc with respect to the geometric center at $\alpha(1950) = 23^{\rm h}21^{\rm m}12.0^{\rm s}$, $\delta(1950) = +58^\circ32'24''$, respectively. Columns 5 and 6 include the LSR velocity and full-width at half maximum, while column 7 lists the size in arc seconds. In those cases where the estimated sizes were of the order of the beam size, and thus could not be accurately determined, only an upper limit of $10''$ is listed. Columns 8 to 10 list the derived mass, column density and number density in terms of the spin temperature (scaled to 50 K) for a distance of 3.3 kpc (Anderson & Rudnick 1995).

Table 1. Observed and derived parameters for H I absorption features associated with Cassiopeia A

H I feature	Central coordinates (1950)						$\Delta\alpha$	$\Delta\delta$	Size	LSR velocity	Δv (FWHM)	Mass	Column density	Number density
	h	m	s	°	′	″	(arcsec)	(arcsec)	(arcsec)	(km s^{-1})	(km s^{-1})	$((\frac{T_s}{50})\,M_\odot)$	$(10^{19}(\frac{T_s}{50})\,\mathrm{cm}^{-2})$	$((\frac{T_s}{50})\,\mathrm{cm}^{-3})$
1	23	20	57.5	+58	31	46.8	−113.7	−37.2	16.2× ≤ 10	−63.9	4.4	< 0.0020	1.4	> 22
2	23	21	3.5	+58	29	52.2	−66.5	−151.8	11.3× ≤ 10	−65.9	7.2	< 0.0030	2.1	> 40
3	23	21	5.5	+58	30	43.7	−50.9	−100.3	11.6 × 13.7	−66.0	∼ 9	0.0024	1.4	23
4	23	21	6.4	+58	30	17.0	−43.8	−127.0	≤ 10× ≤ 10	−66.5	∼ 9	< 0.0030	2.6	> 52
5	23	21	8.5	+58	30	38.5	−27.4	−105.5	23.7 × 10.8	−65.7	4.7	0.0040	1.4	18
6	23	21	8.6	+58	30	31.9	−26.8	−112.1	≤ 10× ≤ 10	−66.3	5.5	< 0.0020	1.4	> 29
7	23	21	9.4	+58	30	6.8	−20.7	−137.2	16.0× ≤ 10	−66.6	3.5	< 0.0020	1.1	> 17
8?	23	21	12.4	+58	31	7.0	3.0	−77.0	≤ 10× ≤ 10	∼ −68	∼ 10	< 0.0010	1.0	> 20
9	23	21	21.0	+58	30	36.0	−70.5	−108.0	20.8× ≤ 10	−62.3	∼ 17	< 0.0070	∼ 3	> 43
10	23	21	23.3	+58	31	0.0	88.5	−84.0	27.7× ≤ 10	−65.3	7.0	< 0.0040	1.4	> 17
11	23	21	24.1	+58	33	19.6	94.7	55.1	15.6× ≤ 10	−68.5	3.7	< 0.0010	0.6	> 10
12	23	21	24.2	+58	32	55.5	95.3	31.5	18.5 × 10.2	−68.7	5.0	0.0015	0.8	11.5
13	23	21	24.7	+58	32	15.0	99.4	−9.0	12.7 × 21.8	−67.6	3.9	0.0008	0.4	4.8
14	23	21	29.3	+58	31	16.0	135.4	−63.6	≤ 10× ≤ 10	−68.0	5.6	< 0.0030	2.7	> 55
15?	23	21	29.3	+58	31	59.9	135.4	−24.1	≤ 10× ≤ 10	−67.2	5.4	< 0.0010	0.9	> 19
16?	23	21	29.9	+58	32	37.8	140.0	13.8	≤ 10× ≤ 10	∼ −63	∼ 10	< 0.00005	∼ 1	> 2
17?	23	21	30.8	+58	33	7.8	147.2	43.8	20.2× ≤ 10	−65.5	∼ 7	< 0.0020	7.4	> 11

The most striking characteristic of the H I absorption knots is their highly asymmetric distribution: all but one of the candidates lie on and beyond the southern and eastern edges of the main SNR shell. To the north no high velocity features are observed, while feature 1 is the only one on the western edge. In addition, the only feature located within the main SNR shell is feature 8, an uncertain source since the τ profile shows only a 2σ feature.

From Fig. 1, a general positional correspondence is apparent between the H I absorption features and the filamentary optical emission, mainly around the SW (features 1 to 8). On the other hand, the correlation between H I absorption features and the continuum maxima is less obvious (Fig. 2). The H I feature 1 is the only concentration which appears projected on a continuum peak. The H I features 2 and 5 are also close to continuum maxima, while features 6 and 15 lie on the edge of continuum peaks. H I absorption knots are also uncorrelated with optical QSFs (van den Bergh & Kamper 1985) and radio knots (Anderson & Rudnick 1995). This lack of correlation, which is observed among the different compact components of Cas A, should not be surprising. Since the physical mechanisms that give rise to the various optical and radio emitting features are probably different, no spatial coincidence is expected.

Another characteristic of these knots is their very low radial velocities. If we assume the systemic velocity of Cas A as $v_{\rm sys} = (-52 \pm 4)$ km s^{-1} (Goss et al. 1988), then the radial velocities $v_{\rm r}$ of the H I knots lie in the range −10 to −17 km s^{-1}. These velocities are much lower than those derived from optical and radio studies for compact features associated with Cas A (typically 4000 to 8000 km s^{-1}, 200 km s^{-1} and 950 km s^{-1} for FMKs, QSFs and radio knots, respectively).

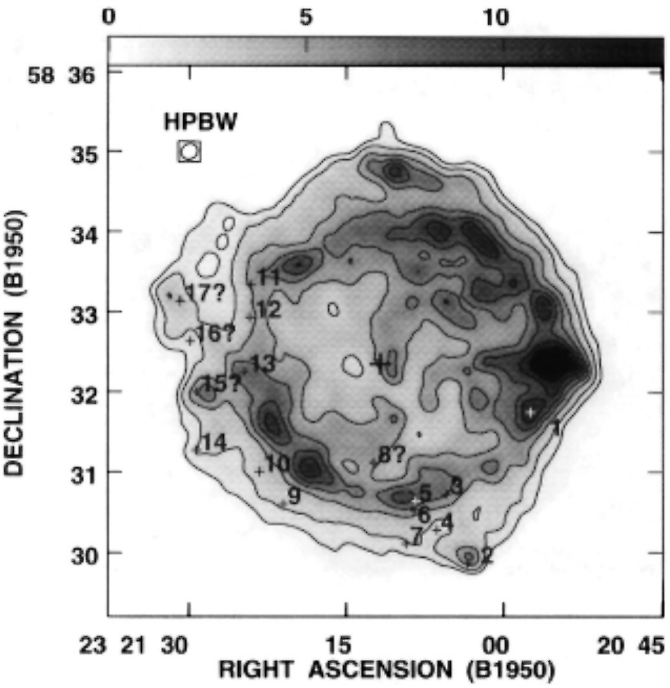

Fig. 2. Greyscale and contour image of the continuum emission of Cas A at 1420 MHz. The greyscale is linear from 0 to 14 Jy/beam. The contours are at 1, 2, 4, 6, 8, 10, 12 and 14 Jy/beam. The beamsize is shown in the top left corner. The positions of the H I absorption features are indicated. The big plus sign at the center shows the location of the assumed geometric center as in Fig. 1

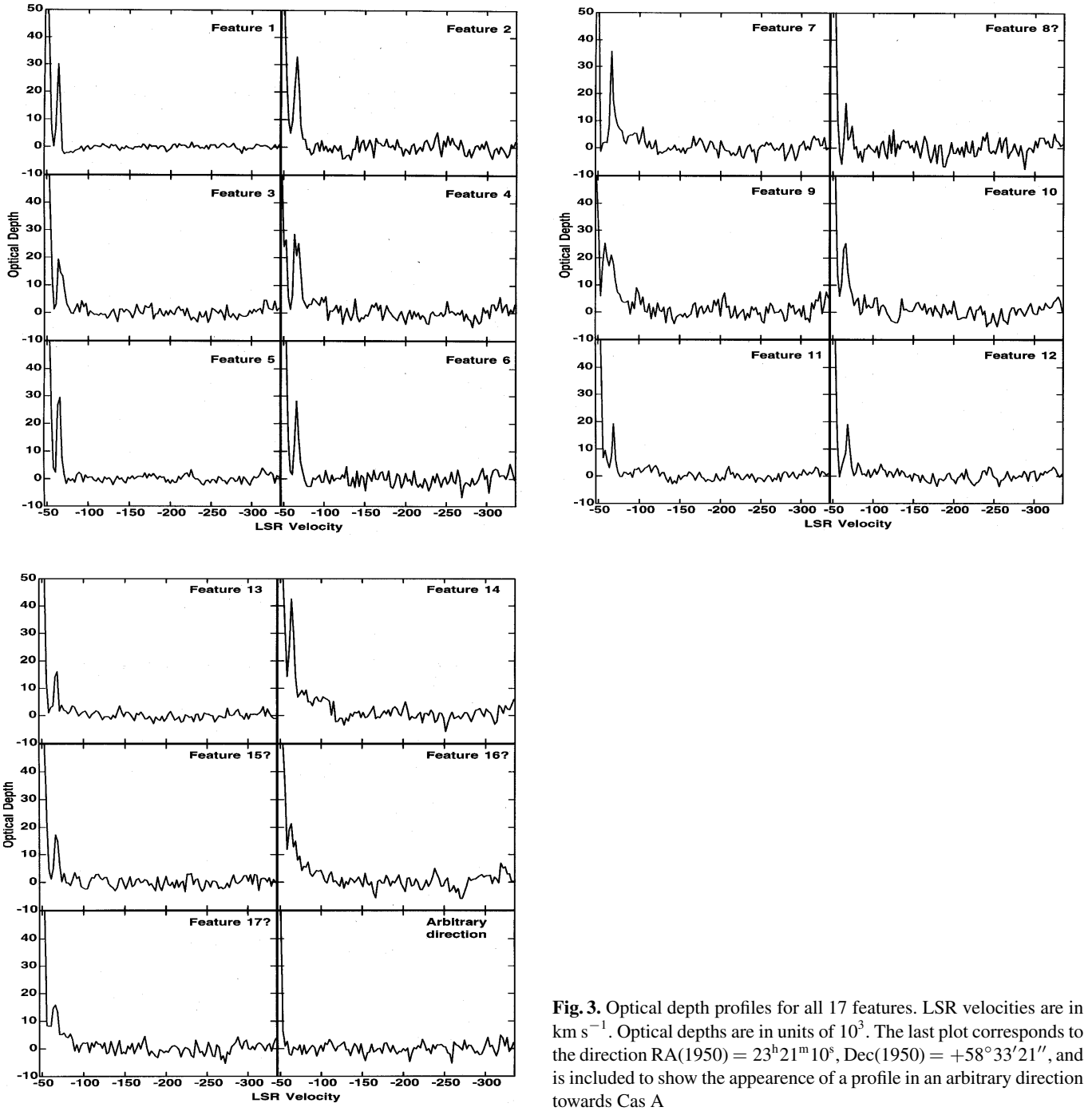

Fig. 3. Optical depth profiles for all 17 features. LSR velocities are in km s^{-1}. Optical depths are in units of 10^3. The last plot corresponds to the direction RA(1950) $= 23^{\rm h}21^{\rm m}10^{\rm s}$, Dec(1950) $= +58^\circ 33' 21''$, and is included to show the appearence of a profile in an arbitrary direction towards Cas A

4. Discussion

4.1. Association of the H I knots with Cas A

In what follows we analyze the likelyhood of a physical association of the observed absorbing H I knots with Cas A. One question to answer is whether the selected knots are distinct entities or if they are related to the Perseus arm gas. Since Cas A itself lies inside the Perseus arm, any associated H I feature with low radial velocity will necessarily appear close in velocity to the gas in the arm. In fact, our observations (Fig. 3) show that the features appear near the velocity range where Perseus arm H I is expected, i.e. from 0 to -55 km s^{-1}, but well separated from it. Therefore, these absorption features can be easily distinguished from the galactic arm contribution.

The appearance of the observed features is clumpy, undoubtedly different from the typical interstellar features, which are generally seen as extended loops, arcs or filaments (Bieging et al. 1991). Moreover, the observations performed by Bieging et al. (1991) and Schwarz et al. (1996) in direction to Cas A covering a broader velocity range, showed no such small, weak features, neither along the near side of the Perseus arm nor in the local H I gas.

Besides, in a similar absorption study performed by Dwarakanath et al. (private communication) in the direction to Cygnus A, using the VLA in the C array over a velocity range spanning approximately from -200 to $+100\,\mathrm{km\,s^{-1}}$, no evidence was found of such small, knotty features, even though the resolution (HPBW $\sim 15''$) and sensitivity (1σ detection limit of about 0.001) were adequate to detect similar features observed here in the direction of Cas A, which have typical opacities higher than 0.02.

In summary, the features around $\sim -65\,\mathrm{km\,s^{-1}}$ in Cas A are apparently unique, suggesting that they are not just standard interstellar concentrations, but have some unusual origin. This hypothesis is additionally supported by the fact that these high velocity features exist only in an unusually narrow velocity range, from -62 to $-69\,\mathrm{km\,s^{-1}}$. Both the location of the H I clumps, projected against Cas A, and the agreement of the LSR velocities of the H I features with the systemic velocity of Cas A, are consistent with the existence of some physical connection between them.

4.2. Comparison with a shocked cloud model

After the first H I absorption high velocity feature in front of Cas A was detected (Goss et al. 1988), the proximity to three prominent QSFs led to the suggestion that this object might be a recombined QSF. Thus, it was assumed that the feature was located on the SNR outer shell and that its velocity was $\sim 100\,\mathrm{km\,s^{-1}}$, typical of QSFs. The low radial velocity observed was ascribed to a projection effect. Under these assumptions, the H I feature was consistent with a model of a small cloud overrun by the SNR shock wave, based on the theory of McKee & Cowie (1975).

Here, we find that such H I absorption knots are quite common over Cas A, and that they all have low observed radial velocities, independent of orientation with respect to the center of Cas A. In order to investigate if these low velocities are due to a projection effect, we have plotted in Fig. 5a) the distance r from each knot to the geometric center of Cas A against their LSR velocities v_{LSR}. LSR velocities can be readily converted into radial velocities v_{r} by subtracting them from $-52\,\mathrm{km\,s^{-1}}$, the assumed systemic velocity of Cas A (Goss et al. 1988). If the knots were distributed over an expanding shell, then shorter distances would correspond to higher radial velocities. Due to the small number of detected features, the tendency shown in Fig. 5a) is not obvious. We cannot conclude whether the knots are expanding on a spherical shell or following a randomized motion. Nevertheless, with the aim of studying the nature of these cold clumps of gas which have been discovered to be moving ahead of Cas A, let us assume that they are uniformly expanding in a spherical shell. If such a shell has a radius R and a uniform expansion velocity V, geometrical considerations imply that r^2 should obey the law $r^2 = R^2 - (R/V)^2 v_r^2$. In Fig. 5b), we have plotted r^2 against v^2. A least squares fit yields $R = 155'' \pm 15''$ (~ 2.5 pc at a distance of 3.3 kpc) and $V = 23 \pm 2\,\mathrm{km\,s^{-1}}$, with a correlation coefficient of 0.45. In what follows, we will use this result as a working hypothesis and

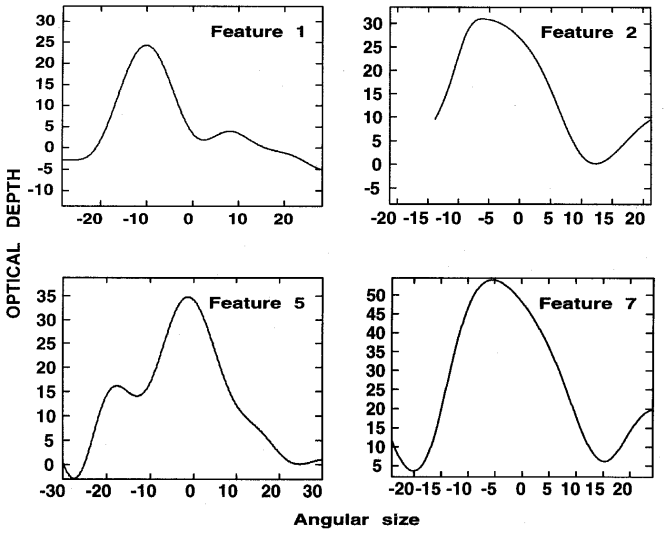

Fig. 4. Spatial cuts (optical depth versus position) for features 1, 2, 5 and 7. Optical depths are in units of 10^3. The secondary peak of feature 5 corresponds to feature 6. The cuts are at position angles $-45°$, $-41°$, $-52°$ and $65°$, respectively, and correspond to the minor axis for features 1 and 5 and to the major axis for features 2 and 7

apply the theory of McKee & Cowie (1975), assuming that real expansion velocities for the knots are of the order of $\sim 23\,\mathrm{km\,s^{-1}}$, as derived from the expanding shell model.

According to McKee & Cowie, if the H I knots are shocked clouds, their densities satisfy a relation:

$$\frac{n_{\mathrm{c}}}{n_0} = 3\left(\frac{v_{\mathrm{b}}}{v_{\mathrm{c}}}\right)^2 , \qquad (1)$$

where n_0 is the pre-shock density, v_{b} the blast wave velocity, n_{c} the cloud density, and v_{c} the cloud velocity. The factor three is the over-pressure in the shocked cloud for the maximum contrast case. The pre-shock density n_0 does not have a unique value for Cas A, since the global asymmetry observed in velocity can be explained if ejecta encounter material on the front face which is denser than material on the back face. Braun (1987) finds that the density varies between 3.7 and $0.4\,\mathrm{cm^{-3}}$, while Reed et al. (1995) conclude that the contrast between front face and back face densities should be as high as five, with $n_0 = 20\,\mathrm{cm^{-3}}$ for the blue-shifted side and $n_0 = 4\,\mathrm{cm^{-3}}$ for the red-shifted side.

The blast wave velocity will also vary depending on the direction of motion. The approaching velocity is expected to be lower than the receding one, since it will be decelerated by denser material. Braun (1987) finds that the blast wave is approaching with a velocity of $v_{\mathrm{b}} \simeq 2300\,\mathrm{km\,s^{-1}}$, and receding with $v_{\mathrm{b}} \simeq 3800\,\mathrm{km\,s^{-1}}$.

Combining the front face density and approaching velocity given by Braun, we obtain $n_{\mathrm{c}} \simeq 6.4 \times 10^7 v_{\mathrm{c}}^{-2}$ which, adopting $v_{\mathrm{c}} = 23\,\mathrm{km\,s^{-1}}$ from our results, yields a cloud density of $\sim 10^5\ \mathrm{cm^{-3}}$, much higher than the observed values, which are $\sim 20(T_{\mathrm{s}}/50)\,\mathrm{cm^{-3}}$ (see Table 1). Note that for those features which are resolved with the $12''$ beam, the derived densities are even lower than $\sim 20(T_{\mathrm{s}}/50)\,\mathrm{cm^{-3}}$. According to Keohane et

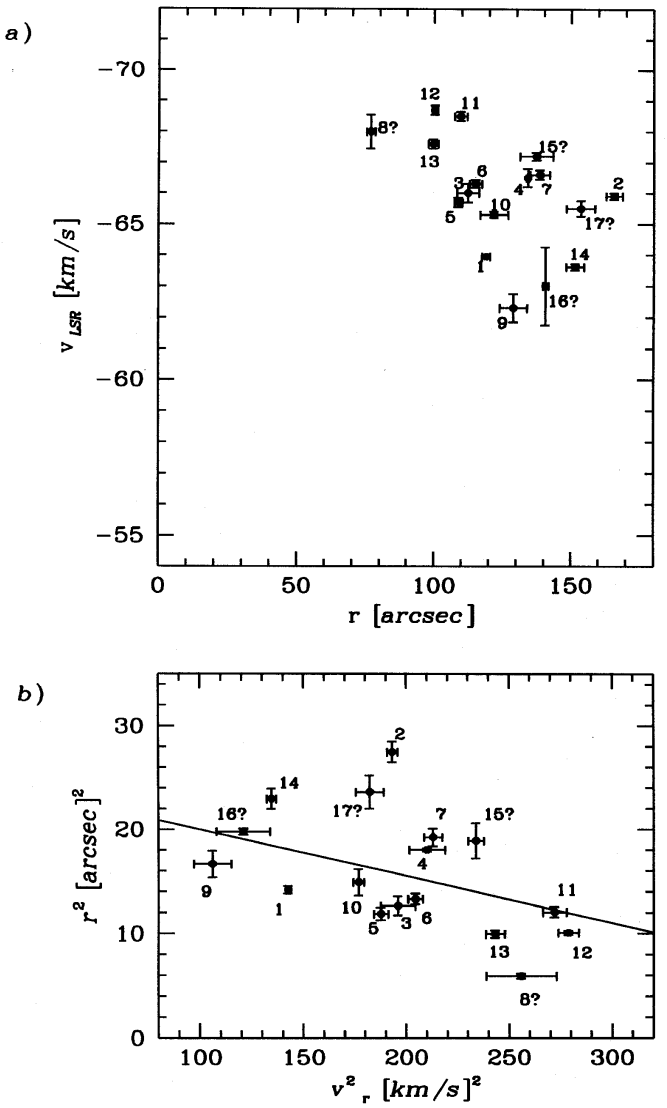

Fig. 5. a LSR velocity of the H I absorption features plotted against their distances to the assumed geometric center of Cas A. Angular distances are measured in arcseconds, **b** Square of the radius with respect to the geometric center is plotted against the square of the radial velocity for the H I absorption features. Radial velocities are measured with respect to the assumed systemic velocity of -52 km s^{-1}. The units of the y axis are 10^3 arcsec^2. In both plots, the error bars indicate the uncertainties of the peak positions in r and of the gaussian fitting in v

al. (1996), the average spin temperature of the H I in the direction of Cas A is ~ 40 K. If we assume that the H I features are recombined shocked clouds, then the spin temperatures could be in the range 100–1000 K, much warmer than the assumed interstellar value. Therefore, the ratio $(T_s/50)$ could be as high as 20 in the extreme case. But even in this case, the measured densities (see Table 1) are not comparable with the density suggested by McKee & Cowie's (1975) model. If we assume that the ambient density is 20 cm^{-3}, as proposed by Reed et al. (1995), the discrepancy is even more dramatic. In summary, it appears that the H I knots detected here are not consistent with a model of pre-existing clouds overtaken by the blast wave.

4.3. The H I knots as material associated with the progenitor star

Since the H I absorption features cannot result from clouds overtaken by the supernova blast wave, we consider models in which they are due to material associated with the progenitor star, but which has not yet been shocked by the blast wave. Such material might have resulted from episodes of stellar mass loss during the late stages of the progenitor evolution.

We first consider the possibility of material from a stellar wind, following the suggestion of Fesen et al. (1987) that the progenitor star of Cas A was a Wolf-Rayet star of the WN-type. Wolf-Rayet stars are strong sources of stellar winds (Barlow 1982) that create interstellar bubbles. Although our H I data show a number of discrete concentrations rather than a uniform shell, we can apply the wind driven bubble model developed by Weaver et al. (1977) as a first approximation, assuming that these H I knots are embedded in a thin H I bubble. In what follows, we discuss the evolutive phase of such a shell and derive physical parameters in order to compare with the observations. The low velocities found here for the H I is a general trend for neutral gas associated with wind blown bubbles. Such low velocity H I bubbles have been observed in emission around several early-type stars (Niemela & Cappa de Nicolau 1991, and references therein).

The adopted stellar mass loss rate is $\dot{M} = 6.3 \times 10^{-5}\ M_\odot$ yr^{-1} and the terminal wind velocity $v_\infty = 1650$ km s^{-1} for the WNL (late) subtype, and $\dot{M} = 3.1 \times 10^{-5}\ M_\odot$ yr^{-1} and $v_\infty = 1900$ km s^{-1} for the WNE (early) subtype (Leitherer et al. 1992, and references therein). We can estimate the time at which radiative cooling begins to be important in a bubble blown by the wind of a WR star as

$$t_c \sim 1.7 \times 10^3 \left(\frac{\dot{M}_6 v_{2000}^2}{n_0}\right)^{1/2} \text{ yrs} \quad (2)$$

(Weaver et al. 1977), where $\dot{M}_6$ is the mass loss rate in units of $10^{-6}\ M_\odot$ yr^{-1}, v_{2000} is the terminal velocity in units of 2000 km s^{-1} and n_0 is the ambient density. Assuming $n_0 = 3.7$ cm^{-3} (Braun 1987), we obtain $t_c \simeq 4.7 \times 10^3$ yrs for a WNE star and $t_c \simeq 5.8 \times 10^3$ yrs for a WNL star. At the cooling time, the radii of the bubbles can be estimated, using the energy conserving phase equations, as

$$R = 28 \left(\frac{\dot{M}_6 v_{2000}^2}{n_0}\right)^{1/5} t_6^{3/5} \text{ pc} \quad (3)$$

(Castor et al. 1975), yielding 2.1 pc for a WNL star and 1.7 pc for a WNE star. Therefore, since the wind driven shell is located beyond 2.1 pc, we can assume that it has already entered the momentum conserving phase and obeys the law

$$R = 28 \left(\frac{L_{36}}{n_0 v_{1000}}\right)^{1/4} t_6^{1/2} \text{ pc} \quad (4)$$

(McCray 1977), where L_{36} is the stellar luminosity, defined as $\dot{M}v_\infty^2$, in units of 10^{36} ergs s^{-1}.

Applying equation (4) with the radius of 2.5 pc obtained in Sect- 3.1 and an initial ambient density of $n_0 = 3.7\,\mathrm{cm}^{-3}$, the age of the bubble is $\sim 8 \times 10^3$ yrs for a WNL-type star, and $\sim 10^4$ yrs for a WNE star. For $n_0 \simeq 20\,\mathrm{cm}^{-3}$ (Reed et al. 1995) the estimated lifetimes are $t \simeq 2 \times 10^4$ yrs and 2.5×10^4 yrs, respectively.

In order to test the proposed model, we independently estimated the bubble age from the position and radial velocities of the H I knots. Since $R \propto t^{1/2}$ in the momentum conserving phase, $t = R/2V$ is $\sim 5 \times 10^4$ yrs, in good agreement with the ages obtained from the wind bubble model. The agreement is closer for a higher initial density. In summary, a scenario where the H I knots are embedded in a tenuous expanding shell about 10^4 years old adequately describes the observations.

Another possibility is that the H I knots are stellar material ejected as dense clumps by the supernova precursor, old enough to be moving ahead of the SN blast wave. Evidence of local enhancements in density in WR winds has been found in optical (Robert & Moffat 1990) and IR spectra (Eenens 1992) for a number of WR stars. The filamentary or clumpy structure shown by several galactic WR rings suggests that a substantial amount of the stellar mass loss from the central star occurs in the form of condensations within the continuous outflow (Moffat & Robert 1992, and references therein). The clumps possibly originate in radiatively-driven instabilities (Poe et al. 1990). Assuming that the clumps were ejected with initial velocities of $\simeq 0.8$ of the wind terminal velocities (Prinja & Smith 1992) and that they were uniformly accelerated to their current positions and velocities as measured in the H I line, we can estimate their dynamical ages to be ~ 3–4×10^3 yrs. On the other hand, if we assume uniform expansion instead of uniform acceleration, we can set an upper limit of 1×10^5 yrs for the age. These estimates are also in rough agreement with the observed parameters.

Taking into account that the duration of the WR phase is about 5×10^5 yrs (Maeder 1991), it can be concluded that the ejection of the H I knots took place long before the explosion and during the WR phase of the progenitor star. Whether the features are condensation nuclei in a cooling wind driven bubble or discrete clumps of stellar ejecta cannot be resolved on the basis of the current observations.

5. Conclusions

The study of the neutral hydrogen absorption in the direction of Cas A led to the discovery of a new kind of compact component which is likely associated with this bright SNR. We have shown the existence of at least 13 H I absorption features in front of Cas A. There are four additional candidates whose reliability is uncertain. These features are thought to be associated with Cas A based on the following arguments: they appear projected against Cas A at peculiar velocities, clearly separated from the normal interstellar gas associated with the Perseus arm; they are present within a very narrow velocity range, which precludes from a standard interstellar origin for the observed features; they have similar shape, size and mass than the optical QSFs associated with Cas A; they do not look like standard interstellar clouds, which generally appear as loops, arcs or filaments; and nothing similar has been ovserved towards Cygnus A, another bright radio source that allows an absorption study.

These features are moving with very low radial velocities with respect to the systemic LSR velocity of the remnant. Many of these features are quite elongated and show substructure. The total mass of the H I gas contained in the H I absorbing knots is less than 0.04 $M_\odot$ (spin temperature of 50 K).

These clumps are preferentially distributed towards the east and south of the radio-continuum shell. The observed asymmetry is compatible with a model where the SE region of the shell is approaching. Such model has been previously proposed for Cas A by Markert et al. (1983) and by Kenney and Dent (1985) based on X-ray and 86 GHz data respectively. We have also shown that the absorbing features depict some spatial correspondence with the diffuse filamentary optical emission (Fig. 1).

There is some evidence that the kinematics of the H I knots can be described by a model in which they are distributed over a ~ 2.5 pc radius shell expanding at about 23 km s^{-1}. Based on this scenario, we have investigated several possible origins for the observed compact H I features. We estimated the age of the H I knots in different ways finding a lower limit of 3 to 4 thousand years. We conclude that the H I clumps must have been ejected before the SN event, probably during the WR stage of the precursor star.

Acknowledgements. This research was partially supported by a Cooperative Science Program between the NSF (USA) and CONICET (Argentina). E. M. R. would like to thank NRAO for support during her visit to the VLA. P. F. W. acknowledges additional support from the NSF through grant AST-9315967 and from the Keck Northeast Astronomy Consortium. We also thank T. Troland, J. Bieging and K. S. Dwarakanath for helpful comments.

References

Anderson M.C., Rudnick L., 1995. ApJ 441, 307
Ashworth W.B., 1980, J. Hist. Astr. 11, 1
Barlow M.J., 1982, in: Wolf Rayet Stars: Observations, Physics, Evolution, C. de Loore, A.J. Willis (eds.). Reidel, Dordrecht, p. 149
Bell A.R., 1977, MNRAS 179, 573
Bieging J.H., Goss W.M., Wilcots E.M., 1991, ApJS 75, 999
Braun R., 1987, A&A 171, 233
Castor J., McCray R., Weaver R., 1975, ApJ 200, L107
Chevalier R.A., Kirshner R.P., 1978, ApJ 219, 931
Chevalier R.A., Kirshner R.P., 1979, ApJ 233, 154
Eenens P.R.J., 1992, ASP Conference Series Vol. 22, Nonisotropic and variable outflows from stars, Drissen L., Leitherer C., Nota A. (eds.), p 145
Fesen R.A., Becker R.H., Blair W.P., 1987, ApJ 313, 378
Goss W.M., Kalberla P.M.W., Schwarz U.J., 1988, in: IAU Colloquium No 101, Supernova Remnants and the Interstellar Medium, Roger R., Landecker T. (eds.). Cambridge University Press, Cambridge, p 239
Kamper K., van den Bergh S., 1976, ApJS 32, 351

Kassim N.E., Perley R.A., Dwarakanath K.S., Erickson W.C., 1995, ApJ 455, L59
Kenney J.D., Dent W.A., 1985, ApJ 298, 644
Keohane J.W., Rudnick L., Anderson M.C., 1996, ApJ, in press
Leitherer C., Robert C., Drissen L., 1992, ApJ 401, 596
Maeder A., 1991, IAU Symp. 143, WR stars and interrelations with other massive stars in galaxies, van der Hucht K.A., Hydayat B. (eds.), p 445
Markert T.H., Canizares C.R., Clark G.W., Winkler P.F., 1983, ApJ 268, 134
McCray R., 1983, Highlights of Astronomy, Vol. 6, West R.M. (ed.), p 565
McKee C.F., Cowie L.L., 1975, ApJ 195, 715
Mebold U., Hills D.L., 1975, A&A 42, 187
Moffat A.F.J., Robert C., 1992, ASP Conference Series Vol. 22, Non-isotropic and variable outflows from stars, Drissen L., Leitherer C., Nota A. (eds.), p 203
Niemela V.S., Cappa de Nicolau C.E., 1991, AJ 101, 572
Peimbert M., van den Bergh S., 1971, ApJ 259, 198
Poe C.H., Owocki S.P., Castor J.I., 1990, ApJ 358, 199
Prinja R.K., Smith L.J., 1992, A&A 266, 377
Reed J.E., Fabian A.C., Winkler P.F., 1991, in Proceedings 10, Santa Cruz Summer Workshop in Astronomy & Astrophysics. Woosley S.E. (ed.), Springer, New York, p 649
Reed J.E., Hester J.J.. Fabian A.C., Winkler P.F., 1995, ApJ 440, 706
Robert C., Moffat A.F.J., 1990, ASP Conference Series Vol. 7, Properties of hot luminous stars, Garmany C.D. (ed.), p 271
Schwarz U.J., Goss W.M., Kalberla P.M., 1996, A&A, submitted
Tuffs R.J., 1986, MNRAS 219, 13
van den Bergh S., 1971, ApJ 165, 457
van den Bergh S., Kamper K., 1983, ApJ 268, 129
van den Bergh S., Kamper K., 1985, ApJ 293, 537
Weaver R., McCray R., Castor J., Shapiro P., Moore R., 1977, ApJ 218, 377